Limnol. Oceanogr., 58(5), 2013, 1640–1656

doi:10.4319/lo.2013.58.5.1640

Microbes, macrofauna, and methane: A novel seep community fueled by aerobic methanotrophy

Andrew R. Thurber,[1,2,*] Lisa A. Levin,[2,3] Ashley A. Rowden,[4] Stefan Sommer,[5] Peter Linke,[5] and Kerstin Kröger[4,a]

[1] College of Earth, Ocean, and Atmospheric Sciences, Oregon State University, Corvallis, Oregon
[2] Integrative Oceanography Division, Scripps Institution of Oceanography, University of California, San Diego, La Jolla, California
[3] Center for Marine Biodiversity and Conservation, Scripps Institution of Oceanography, University of California, San Diego, La Jolla, California
[4] National Institute of Water and Atmospheric Research, Wellington, New Zealand
[5] Helmholtz Centre for Ocean Research Kiel (GEOMAR), Kiel, Germany

Abstract

During the discovery and description of seven New Zealand methane seep sites, an infaunal assemblage dominated by ampharetid polychaetes was found in association with high seabed methane emission. This ampharetid-bed assemblage had a mean density of 57,000 ± 7800 macrofaunal individuals m^{-2} and a maximum wet biomass of 274 g m^{-2}, both being among the greatest recorded from deep-sea methane seeps. We investigated these questions: Does the species assemblage present within these ampharetid beds form a distinct seep community on the New Zealand margin? and What type of chemoautotrophic microbes fuel this heterotrophic community? Unlike the other macro-infaunal assemblages, the ampharetid-bed assemblage composition was homogeneous, independent of location. Based on a mixing model of species-specific mass and isotopic composition, combined with published respiration measurements, we estimated that this community consumes 29–90 mmol C m^{-2} d^{-1} of methane-fueled biomass; this is > 290 times the carbon fixed by anaerobic methane oxidizers in these ampharetid beds. A fatty acid biomarker approach supported the finding that this community, unlike those previously known, consumes primarily aerobic methanotrophic bacteria. Due to the novel microbial fueling and high methane flux rates, New Zealand's ampharetid beds provide a model system to study the influence of metazoan grazing on microbially mediated biogeochemical cycles, including those that involve greenhouse gas emissions.

Bacteria and Archaea provide a key ecosystem service by mitigating the release of the greenhouse gas methane (Sommer et al. 2006; Reeburg 2007). At deep-sea cold seeps, this service leads to methane-fueled chemosynthetic production and supports unique metazoan communities, adding to the biodiversity of continental margins (Cordes et al. 2010). Yet our understanding of the interplay among metazoan fauna, microbial population structure, and the biogeochemical processes that the microbes facilitate is still in its infancy. Although recent advances have identified how symbiont-bearing fauna affect the sediment-microbial community (Dattagupta et al. 2008), the effects of heterotrophic fauna and "top-down forcing" on seep microbial communities remains largely unknown. Recently, an unusual seep assemblage with abundant ampharetid polychaetes was discovered at the Hikurangi Margin off New Zealand (N.Z.; Baco et al. 2010; Sommer et al. 2010). Initial studies found methane-derived carbon to fuel this infaunal assemblage, providing a pertinent system to study how metazoan food webs interact with microbial communities and production (Thurber et al. 2010). We build upon the initial reports to assess whether this assemblage forms a distinct seep community, characterize its density and composition, and identify what microbial processes fuel this infaunal community.

Sedimented cold seeps consist of a mosaic of distinct habitats commonly identified by a dominant faunal group. These habitats include microbial mats, vesicomyid clam beds, frenulate fields, mussel beds, and vestimentiferan bushes; each differs in geochemistry as well as microbial and metazoan community composition (Levin 2005; Bernardino et al. 2012). Microbial mats are fueled by the greatest flux of methane (up to 100 mmol m^{-2} d^{-1}; Tryon and Brown 2001; Levin et al. 2003; Sommer et al. 2010), whereas clam beds have comparatively reduced and/or oscillating fluid flow (0.2–1.1 mmol m^{-2} d^{-1}; Tryon and Brown 2001; Levin et al. 2003; Sommer et al. 2006) and frenulate fields have even lower methane flux rates (< 0.7 mmol m^{-2} d^{-1}; Sommer et al. 2009). Mud volcanoes, a habitat similar to methane seeps, can have higher flux than seeps, well over 100 mmol m^{-2} d^{-1} (Reeburg 2007) and also include many of the same habitats including frenulate fields (Niemann et al. 2006); however, mud volcanoes have different surface manifestations and traditionally have been treated separately from seeps (Reeburg 2007). Comparable data do not exist for vestimentiferan bushes or mussel beds at seeps. Methane is respired initially through a syntrophic partnership between anaerobic methane-oxidizing Archaea and sulfate-reducing bacteria (reviewed in Knittel and Boetius 2009), resulting in hydrogen sulfide production (Reeburg 2007; Knittel and Boetius 2009). This sulfide can

* Corresponding author: athurber@coas.oregonstate.edu

[a] Present address: Federal Agency for Nature Conservation, Island of Vilm, Pitbus, Germany

be aerobically oxidized by a variety of bacteria, including large sheath-forming bacteria of the genera *Beggiatoa* or *Thioploca*, whose appearance gives microbial mats their name. Methane that is not consumed anaerobically is respired aerobically by both free-living and symbiotic bacteria or released into the hydro- or atmosphere. Together with the anaerobic methane oxidizers, aerobic methane-oxidizing bacteria mitigate the majority of methane release (Murase and Frenzel 2007; Reeburg 2007; Ding and Valentine 2008) by forming the "benthic sediment filter" (Sommer et al. 2006). Although both aerobic and anaerobic processes remove methane, the dominant sink for methane from deep-sea methane seeps sediment is thought to be anaerobic (Reeburg 2007; Knittel and Boetius 2009).

In addition to distinct chemical environments, seep habitats support specialized heterotrophic metazoan assemblages composed of species that can tolerate the associated productive but physiologically stressful conditions. Microbial mats are fueled by millimole levels of sulfide, a compound that is toxic to many eukaryotic taxa (Somero et al. 1989). This toxicity leads to communities dominated by those fauna that can tolerate such chemical stress, including dorvilleid, capitellid, and ampharetid polychaetes, and vesicomyid bivalves (Sahling et al. 2002; Levin et al. 2003, 2013). The reduced chemical stress in clam beds, partially ameliorated by the bioirrigation of vesicomyid bivalves, allows species that are not as tolerant of sulfide to inhabit these communities and penetrate deeper into the sediment; here species from the background community overlap with seep specialists (Levin et al. 2003, 2010). Thus, macrofaunal species composition and vertical distribution within the sediment reflect the biogeochemical, fluid flow, and microbial environment (Sahling et al. 2002; Levin 2005; Menot et al. 2010). As these communities consume the diverse microbes within the sediment, knowledge of which prokaryotes fuel the heterotrophic metazoan community provides insight into the dominant forms of chemical cycling within seep sediments.

The main technique that has been used to identify the type of chemosynthesis-based energy consumed by these communities is stable isotopic analysis (Van Dover et al. 2007), although fatty acid (FA) analysis can provide additional information as to the diet of different species (Dalsgaard et al. 2003). Due to enzymatic preferential incorporation of ^{12}C over ^{13}C, both metabolic substrate and fixation pathways impart a distinctive, although sometimes overlapping, carbon isotopic signature. When organic matter is ingested and assimilated, its signature is retained in consumer tissues with minimal trophic enrichment of ^{13}C, resulting in a biomarker that can resolve dietary sources. This technique has been successfully used to identify metazoan use of chemosynthetic production (Eller et al. 2005; Deines et al. 2007). Yet the relative importance of specific metabolic substrates is difficult to resolve since in many cases an intermediate value can either be indicative of a mixed diet of two sources or a third source entirely. FA signatures offer an alternative technique for studying food web linkages (Dalsgaard et al. 2003). As constituents of bacterial and eukaryotic lipids, FAs have characteristic branching and distribution of double bonds that loosely follow taxonomic lineages within producers. FA profiles of consumers reflect a combination of items incorporated directly from their diets and those synthesized by the consumer along known pathways. Importance of bacterial production or recycling has been demonstrated through FA analysis, and this technique has begun to be employed more extensively to identify the heterotrophic interactions at methane seep ecosystems (MacAvoy et al. 2003; Van Gaever et al. 2009; Thurber et al. 2012).

Multiple sites of methane seepage were recently discovered along the N.Z. margin (Baco et al. 2010; Greinert et al. 2010), but microbial mats were conspicuously absent. Instead, ampharetid polychaetes were found in abundance in areas of the most intense seepage (Baco et al. 2010; Sommer et al. 2010; *see* Barnes et al. 2010 for a treatment of the underlying geology of these sites). The ampharetids themselves belonged to two distinct and novel genera, contained functional guts, and were observed to surface-deposit feed. They did not appear to have any symbionts (Sommer et al. 2010). In these ampharetid beds, local methane flux was more than double that previously observed in any other seep habitat (Sommer et al. 2010), excluding mud volcanoes. Metazoans present in the ampharetid beds gained between 6% and 100% of their energy from methane-derived carbon, based on stable isotope analyses (Thurber et al. 2010; Dale et al. 2010). This observation, combined with the high rate of methane flux, suggested that the ampharetid beds may be a distinct community with respect to both nutritional source and metazoan composition. In this study we describe the faunal composition of the macroinvertebrate assemblage within the seep habitat and couple FA analysis to an isotopic, mass-based model to answer the questions:

(1) Does the species assemblage present within these ampharetid beds form a distinct seep community on the N.Z. margin?
(2) Which microbial processes provide nutrition for the heterotrophic species in the ampharetid-bed communities?
(3) What is the rate of microbial methane oxidation required to fuel the ampharetid-bed communities?

In light of these questions, we also consider how this seep assemblage compares globally to known seep assemblages in terms of infaunal density, biomass, and methane flux.

Methods

Sample collection and processing—Methane seep sediments were sampled aboard R/V *Tangaroa* (cruise TAN 0616; 05–18 November 2006) and R/V *Sonne* (cruise SO 191-3; 22 February–14 March 2007) along New Zealand's North Island (Fig. 1; Table 1). Together seven sites at three different locations were sampled by a total of eight "blind" and 14 video-guided multicorer deployments between 662 m and 1172 m water depth. These samples were used to quantify assemblage structure and similarity and faunal

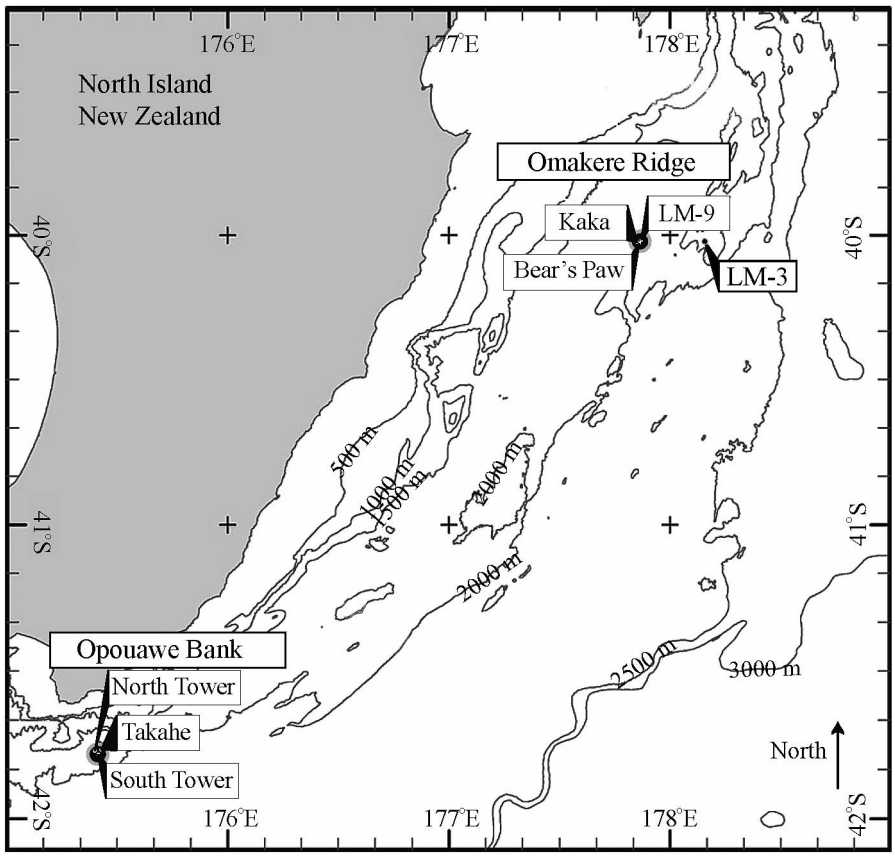

Fig. 1. Sampling locations of methane seeps off the North Island, New Zealand. Contour lines = 500 m. Figure modified from Baco et al. 2010. For fine-scale maps of each sampling location, please *see* Greinert et al. 2010.

Table 1. Study locations, sites, macrofaunal density, and number of fatty acid (FA) analyses run from each site. Mean carbon stable isotopic signature of all individuals with standard error (SE) and sample size given, and the wet-weight biomass of two samples. Stations in bold are ampharetid-bed sites and the station in italics was a "non-seep" habitat.

Location	Site	Station	Density (n m^{-2})	FA (n)	Stable isotopic signature δ^{13}C ± SE (n)	Mass (g m^{-2})
Omakere Ridge	LM-9	46		3	−25.7±1.2 (12)	
	LM-9	49	6540		−23.8±1.6 (3)	
	LM-9	54	7225			
	LM-9	57	7336		−30.5±2.0 (19)	
	Kaka	**261**	73,848	7	−35.6±1.9 (28)	201
	Kaka	262	6451			
	Kaka	242	39,088	5	−29.5±0.9 (31)	
	Kaka	232		5	−33.2±1.7 (15)	
	Bear's Paw	186	5475	2	−37.6±1.8 (13)	
	Bear's Paw	195		3	−44.3±3.1 (8)	
	Bear's Paw	**196**	65,317	16	−46.4±1.6 (45)	273
LM-3	LM-3	**216**	33,486	4	−52.5±1.7 (21)	
	LM-3	**259**	39,980			
	LM-3	*260*	4669			
Opouawe Bank	North Tower	84	14,009	2	−19.4±0.6 (9)	
	North Tower	86	22,670		−24.7±1.3 (11)	
	North Tower	112	25,543		−20.6±0.9 (21)	
	North Tower	**290**	49,274	5	−48.7±3.1 (12)	
	North Tower	291	32,149			
	South Tower	116	28,459		−27.2±1.1 (11)	
	Takahe	309		17	−37.9±1.0 (64)	
	Takahe	**315**	81,615			

stable isotopic and FA composition; however, due to core limitations not all analyses were able to be performed on specimens from each multicorer deployment. Blind cores sampled a continuum between seep and non-seep habitats and video-guided multicorers targeted ampharetid beds exclusively. Between one and three cores from each of the 18 successful multicorer deployments were preserved in 8% formalin for quantitative community analysis. The top 5 cm were vertically fractioned into 0–1, 1–2, 2–3, and 3–5 cm layers and preserved unsieved. Three remaining sediment fractions, 5–7, 7–10, and 10–20 cm, were sieved on a 300 μm mesh prior to preservation. After return to the laboratory, all sediment sections were sieved on a 300 μm sieve, and the fauna was identified to the lowest possible taxon and counted separately for each depth layer. All multicorer deployments were made in as close proximity as possible to methane seeps, except at Sta. 260 where cores were collected away from seepage activity to provide a reference station.

Additional tubes from each of those multicorer deployments, as well as samples from multicorer deployments that did not yield quantitative samples, were sieved on a 300 μm sieve and sorted live at sea; animals found in these were used for stable isotopic and FA analysis. FA composition was analyzed for 69 individuals taken from 11 multicorer deployments at seven sites (Table 1). Six of these multicorer deployments and 49 of the individuals analyzed for FA were from ampharetid beds. A total of 323 individuals were analyzed for stable isotopic composition with 170 of those individuals from ampharetid beds. Individuals for FA and stable isotopic analyses were placed in 25 μm filtered seawater overnight to allow gut evacuation. They were then placed in preweighed tin boats for stable isotopic analysis or cryovials for FA analysis before being frozen at -20°C or -80°C, respectively. Treatment of stable isotopic samples is described in Thurber et al. (2010), and samples were analyzed on either a Eurovector elemental analyzer interfaced with a continuous flow Micromass Isoprime isotope ratio mass spectrometer at Washington State University or with a Thermo Finnigan Delta XP Plus with a Costech 4010 Elemental Analyzer at the Scripps Institution of Oceanography analytical facility. All isotope samples were run without lipid extractions and were acidified using 1 mol L^{-1} HCl and 10% $PtCl_2$ acid. Isotope ratios are expressed as $\delta^{13}C$ in units of per mill (‰) in reference to the standard Pee Dee Belemnite. Samples for FA extraction were placed in muffle-furnaced, washed, and pre-extracted glass vials, frozen, and then extracted following the one-step extraction–saponification method of Lewis et al. (2000) as specified in Thurber et al. (2012). Blanks were run concurrently with all samples, and solvents used were American Chemical Society grade or better. Due to the small biomass of all samples, gas chromatography–mass spectrometry was used to measure FA composition due to its high sensitivity. Use of this procedure means that whereas comparisons of relative FA composition within this study are valid, they cannot be directly, quantitatively compared to FA composition in other studies. Standards run throughout the analysis had no shift in the magnitude of relative peak height or area, indicating the validity of this approach. Peaks were identified using a combination of dimethyl-disulfide adduct formation, comparison to known standards (Supelco 37 Component Fatty Acid Methyl Ester mix and Supelco Bacterial Acid Methyl Ester mix, Sigma-Aldrich), and mass spectra. Analysis of peak area was performed using Xcaliber software (Thermo Scientific) based on total spectra and manually checked to confirm accurate peak extent.

Data analysis—Assemblage structure and FA composition of individuals underwent multivariate analysis to identify differences among assemblages or diet differences among individuals. To best characterize the fauna of a given site, the mean macrofaunal community structure of three multicorer tubes from within each deployment was taken in 13 of the 18 deployments. These sample data were analyzed using statistical routines in the multivariate software package Primer-E version 6 (Clarke and Gorley 2006). Bray–Curtis similarity was used to compare samples after square root transformation of abundance data (made to reduce the influence of the highly abundant taxa), and a group average hierarchical clustering routine (CLUSTER) and similarity profile (SIMPROF) permutation tests were used to identify sample groupings. The advantage of the SIMPROF test is that it looks for statistically significant (level set at $p = 1\%$) evidence of genuine clusters of samples (i.e., communities) rather than using an arbitrary cutoff of similarity to define sample groups (Clarke et al. 2008). A multidimensional scaling (MDS) ordination plot was used to visualize the similarity relationship among samples and groups. The strength of the identified groups was evaluated using analysis of similarity (ANOSIM), and the taxa that characterized and discriminated these groupings were identified using similarity percentage (SIMPER) analysis. We report the taxa that contributed at least 10% to the similarity or dissimilarity of the groupings.

To identify the microbial food sources consumed by N.Z. species, individuals with similar diets, based on their FA distribution, were grouped using an alternate multidimensional approach. We based our analysis on individuals rather than the means within cores as different species provide a different level of de novo synthesis (Kelly and Scheibling 2012) and individuals within cores can have very different trophic histories due to vertical position within the core, their trophic guild, or recruitment history (tissues of recent recruits may not reflect a seep-based diet). Therefore, either taking the mean of a species within a single core or the mean of all fauna from the entire core can skew the interpretation of the overall food sources, and variance thereof, consumed within a seep. By using the techniques described here, we gain a more complete understanding of the diversity and variance of trophic fueling at the seep. The FA composition of individuals were $\log(x + 1)$ transformed (to increase the homogeneity of variance within each FA distribution) and compared, also using Bray–Curtis similarity. The CLUSTER routine was used to identify groups by systematically and iteratively varying the similarity cutoff until we found a percent similarity that had a significantly greater variance among groups than within groups as identified by an ANOSIM analysis

($\alpha = 0.05$). Using this iterative-ANOSIM-similarity approach, we found that a 59% similarity cutoff resulted in statistically different groups within the FA data set. An MDS ordination plot was used to visualize the similarity relationship among individuals and groups of individuals. The FAs that characterized and discriminated these groups were identified using SIMPER; again, we report on the four FAs that contribute most (> 10% similarity or dissimilarity) to forming these patterns. An analysis of variance (ANOVA) was employed to test whether the individuals (or co-occurring individuals of the same species) belonging to the groups identified by the iterative-ANOSIM-similarity FA analysis, had $\delta^{13}C$ signatures that were also more similar within rather than among the groups identified by the FA profile. A Tukey post hoc test identified pair-wise differences, and homogeneity of variance was tested graphically.

For two cores, species-specific biomass was measured to allow estimates of the rate of microbial methane oxidation required to fuel the ampharetid-bed communities. These cores, collected from Sta. 196 and Sta. 261, were chosen based on availability of species-specific isotopic data. Since we measured only two cores, and they were among the most dense assemblages sampled, these results should be treated as maximum values for the ampharetid-bed communities rather than characteristic of all ampharetid beds sampled. To measure biomass, formalin-fixed samples were sorted to putative species, placed on preweighed Nitex screen, and blotted to remove excess water before being weighed. For small samples, triplicate measurements were made with rewetting in-between; this leads to reproducible results. Putative species were identified at sea for samples destined for isotope analyses. Resulting data allowed application of a two-source mixing model to estimate the amount of methane-derived carbon used by the ampharetid-bed assemblage. For those species lacking isotope data, the mean of all individuals within the same core was used; however, this was only necessary for 12% and 2% of the species (by biomass) present within cores 261 and 196, respectively. To identify the relative input of methane to the food web, we employed the two-source mixing model of Fry and Sherr (1984) as employed in Thurber et al. (2010) using the equation $F_m = (\delta_I - \delta_{S1})/(\delta_{CH_4} - \delta_{S1})$, where F_m is the percent animal biomass derived from methane, δ_I is the isotopic composition of the animals (I = infauna), δ_{S1}, where S1 equals Source 1, is the upper bound of the mixing model which was either the composition of sulfide-oxidizing bacteria ($\delta^{13}C = -34‰$ or $-28‰$) or particulate organic carbon from this location, and δ_{CH_4} is the isotopic composition of methane with both extreme values measured at this location used ($\delta^{13}C_{CH_4} = -65‰$ or $-60‰$). By changing the endpoints of the mixing model to encompass the widest possible estimates, we can estimate the maximum and minimum values of methane-derived carbon consumed by an individual (but *see* Thurber et al. 2010 for a more in-depth description of biases of mixing-model approaches). We used the respiration rate of ampharetid polychaetes as a proxy for whole assemblage respiration rate (0.29 mmol O_2 g^{-1} min^{-1}, mass in wet weight as measured by Sommer et al. 2010) as they comprised 83% and 62% of the community biomass at Sta. 196 and Sta. 261, respectively. Respiration was converted to carbon utilization using a 0.85 respiratory quotient (Smith 1987). This daily carbon utilization was combined with the species-specific estimate of methane-derived carbon, to model the amount of methane-derived microbial carbon consumed by the ampharetid-bed assemblage on a per-meter and daily bases. By assuming 100% trophic efficiency and applying no carbon trophic fractionation, we have made our estimate of carbon consumed a highly conservative, minimum value.

Results

Assemblage structure—A total of 10,406 individuals were collected from 18 multicorer deployments at seven sites (Table 1). We used the macrofaunal community structure from those multicorer deployments to test if the ampharetid-bed fauna formed a distinct seep community that was homogeneous in composition independent of location. The SIMPROF analysis resulted in three strongly distinct sample groupings and two samples that were grouped individually (A_c–E_c; Global ANOSIM $R = 0.912$; Fig. 2). Within these groupings, Group A_c was most dissimilar to Groups C_c and D_c, respectively, and was always > 55% dissimilar from the remaining groups (SIMPER, Table 2). The main faunal component that separated Group A_c from the remaining groups was the abundance of ampharetid polychaetes (SIMPER, Table 2). All of Group A_c samples had ampharetid densities > 18,000 individuals m^{-2} (Table 3). Samples from Groups B_c, C_c, and E_c had < 170 ampharetids m^{-2}. Group D_c (Sta. 242) had an ampharetid density of 2844 m^{-2}. With the exception of Group A_c, samples from similar locations grouped with each other (Fig. 2). Group E_c samples were all from the Opouawe Bank and Group C_c came from Omakere Ridge. In contrast, Group A_c formed a distinct cluster that included samples from Kaka, LM-3, Takahe, Bear's Paw, and North Tower. We thus conclude here, for ease of further reporting, that Group A_c, the ampharetid beds, are a distinct community among those habitats we sampled on the N.Z. margin.

The ampharetid-bed communities were dominated by two undescribed species, each belonging to a different and novel genus, of the polychaete family Ampharetidae. Mean ampharetid-bed macrofaunal density was 57,000 individuals m^{-2} with the ampharetids making up an average of 25,000 individuals m^{-2} (Table 3). Both of the ampharetid species were present in all of the ampharetid-bed samples with one of the species making up 72% of the Ampharetidae and the other 22%; the remaining 6% could not be identified to the species level. In the macrofaunal sample with the highest density, the infaunal community reached 82,000 individuals m^{-2}, where 33,000 of those individuals were ampharetids. The second two most abundant polychaete families within this community were Dorvilleidae and Spionidae, which had mean densities of 6000 individuals m^{-2} and 2000 individuals m^{-2}, respectively. Cumaceans and a variety of species of gammarid amphipods were more abundant than either of these two polychaete taxa,

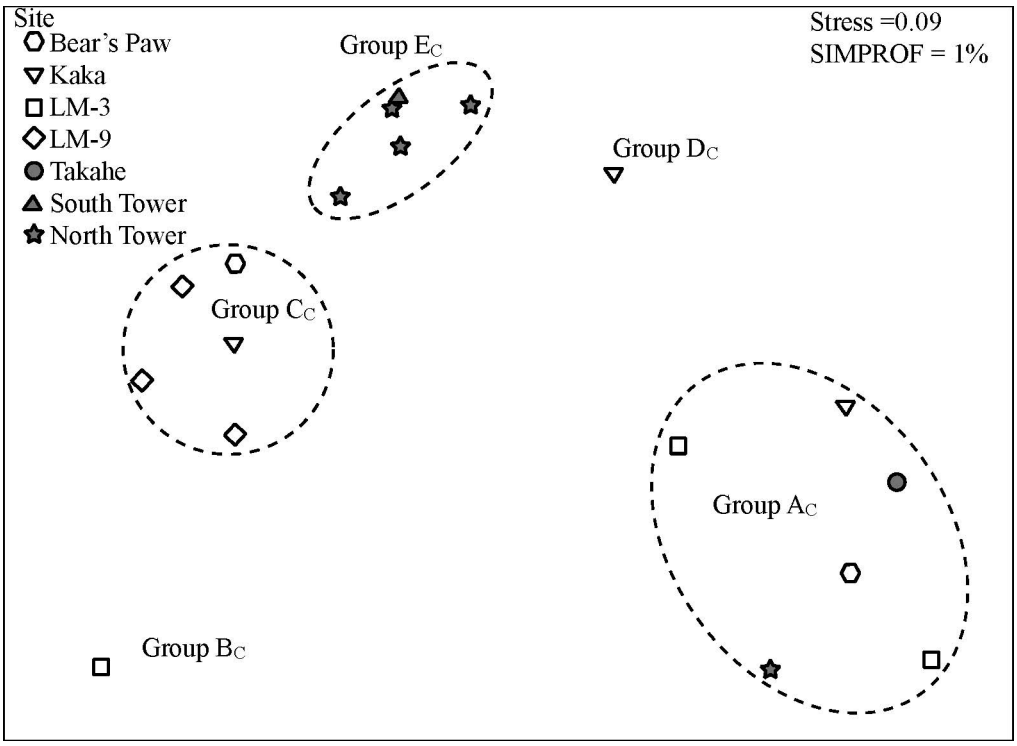

Fig. 2. A 2D representation of the similarity of N.Z. methane seep infaunal communities. Significant different groupings as tested by SIMPROF at 1% and indicated by dotted lines. Those species that drive the groupings are reported in Table 2.

Table 2. SIMPER results indicating which macrofaunal taxa characterized or discriminated the groupings identified in Fig. 2. Total percent similarity or dissimilarity between groups is given in bold. Values indicate the contribution of the indicated fauna to the similarity or dissimilarity of the group. Visualizations of the groupings are displayed in Fig. 2. na, not applicable.

	Group A_c		Group B_c		Group C_c		Group D_c		Group E_c	
Group A_c	**Σ Similarity**	**58**	**Σ Dissimilarity**	**78**	**Σ Dissimilarity**	**71**	**Σ Dissimilarity**	**55**	**Σ Dissimilarity**	**65**
	Ampharetidae	37	Ampharetidae	19	Ampharetidae	22	Ampharetidae	12	Ampharetidae	17
	Gammaridea	16	Cumacea	10	Cumacea	9	Paraonidae	9	Cumacea	7
	Cumacea	14	Gammaridea	10	Gammaridea	9	Amphinomidae	7	Dorvilleidae	7
	Dorvilleidae	11	Dorvilleidae	9	Dorvilleidae	8	Cumacea	6	Gammaridea	5
Group B_c			**Similarity**	**na**	**Σ Dissimilarity**	**51**	**Σ Dissimilarity**	**69**	**Σ Dissimilarity**	**64**
					Oweniidae	8	Dorvilleidae	10	Spionidae	9
					Tanaidacea	5	Amphinomidae	8	Gammaridea	7
					Porifera	4	Paraonidae	8	Tanaidacea	5
					Sabellidae	3	Spionidae	5	Ophellidae	5
Group C_c					**Σ Similarity**	**61**	**Σ Dissimilarity**	**56**	**Σ Dissimilarity**	**48**
					Tanaidacea	11	Dorvilleidae	12	Spionidae	9
					Gammaridea	9	Paraonidae	9	Gammaridea	7
					Spionidae	9	Amphinomidae	9	Bivalvia	5
					Isopoda	8	Ampharetidae	7	Glyceridae	5
Group D_c							**Σ Similarity**	**na**	**Σ Dissimilarity**	**43**
									Dorvilleidae	12
									Ampharetidae	7
									Amphinomidae	7
									Paraonidae	7
Group E_c									**Σ Similarity**	**68**
									Spionidae	13
									Gammaridea	10
									Tanaidacea	8
									Isopoda	7

Table 3. Composition of infaunal communities along the N.Z. margin. Group A is the ampharetid-bed community. Number of stations is given in parentheses and standard errors are among stations (not cores within multicorer deployment). Abundance is given per m^{-2} basis as extrapolated from 75.4–78.5 cm^2 samples.

	Group A_c (6)	Group B_c (1)	Group C_c (5)	Group D_c (1)	Group E_c (5)
Polychaeta					
Acrocirridae	0±0	42	0±0	0	0±0
Ampharetidae	24,885±4783	127	60±37	2844	57±26
Amphinomidae	361±163	0	35±26	4669	603±254
Capitellidae	665±419	0	87±37	42	395±221
Chaetopteridae	0±0	0	9±9	0	0±0
Cirratulidae	7±7	255	384±87	42	248±77
Cossuridae	14±14	0	34±16	1316	345±65
Dorvilleidae	6005±2710	0	27±18	7088	65±36
Enucida juv.	0±0	0	13±13	0	0±0
Fauvelopsidae	0±0	85	18±11	297	0±0
Flabelligeridae	0±0	0	35±16	42	75±41
Fragments	0±0	0	0±0	0	0±0
Glyceridae	85±42	85	17±11	42	770±155
Hesionidae	0±0	42	98±72	0	180±50
Hirudinea	0±0	0	9±9	0	13±13
Lumbrineridae	7±7	0	83±31	127	118±28
Maldanidae	14±9	0	109±42	0	268±72
Nephtyidae	0±0	0	39±11	0	9±9
Nereididae	7±7	0	26±18	127	0±0
Oligochaeta	7±7	85	317±138	1146	526±198
Onuphidae	0±0	85	0±0	0	27±27
Opheliidae	21±21	0	143±19	297	1126±218
Orbiniidae	205±148	0	68±48	424	170±71
Oweniidae	0±0	1188	137±107	42	27±18
Paraonidae	424±408	255	199±71	6833	1563±588
Phyllodocidae	0±0	0	53±32	0	80±49
Pilargidae	0±0	0	13±13	0	43±23
Pisionidae	0±0	0	9±9	0	0±0
unid. Polychaete	78±61	42	83±38	42	92±39
Polynoidae	35±23	0	56±31	0	206±60
Sabellidae	7±7	382	66±17	42	48±34
unid. Scale worm	0±0	0	9±9	42	27±27
Scalebrigmatid	0±0	42	8±8	0	57±16
Siboglinidae	283±258	42	278±246	0	168±168
Sigalionidae	0±0	42	13±13	0	18±18
Sphaerodoridae	0±0	85	8±8	42	53±26
Spionidae	2030±1144	212	519±64	3438	5560±1311
Sternaspidae	0±0	0	0±0	0	9±9
Syllidae	57±57	340	246±109	212	106±63
Terrebellidae	0±0	42	39±17	0	71±36
Trichobranchidae	0±0	0	0±0	42	44±24
Crustacea					
Acari	0±0	0	9±9	0	0±0
Caprellidae	0±0	0	0±0	42	0±0
unid. Crustacea	0±0	0	13±13	0	97±77
Cumacea	9196±3633	85	473±219	2546	479±179
Decapoda	7±7	0	0±0	0	0±0
Gammeridea	9549±3558	170	626±107	1570	3720±800
Isopoda	608±290	127	485±111	764	1556±286
Pycnogonida	14±9	0	0±0	0	0±0
Stomatopoda	7±7	0	0±0	0	0±0
Tanaidacea	545±486	127	817±110	1698	2435±682
Cnidaria					
Anemone	0±0	42	0±0	0	0±0
unid. Cnidaria	0±0	0	17±17	0	97±87
Hydrozoa	0±0	0	0±0	0	80±80

Table 3. Continued.

	Group A_c (6)	Group B_c (1)	Group C_c (5)	Group D_c (1)	Group E_c (5)
Echinodermata					
Asteroidea	0±0	0	0±0	0	13±13
Echinoidea	0±0	0	13±13	0	9±9
Holothuroidea	0±0	0	70±41	0	115±83
Ophiuroidea	0±0	85	34±34	0	117±65
Mollusca					
Aplacophora	7±7	0	79±22	424	53±26
Bivalve	127±46	85	141±74	806	1366±293
Patellogastropoda	71±42	0	0±0	0	0±0
Prosobranchia	842±833	85	26±17	85	39±17
Scaphopoda	0±0	0	34±25	42	272±156
Solemyidae	50±35	0	0±0	637	22±14
Other					
Nemertea	1004±555	127	364±146	1146	675±216
Phoronida	0±0	0	0±0	0	9±9
Platyhelminthes	21±21	0	0±0	0	18±11
Porifera	0±0	255	13±13	0	0±0
Priapulida	0±0	0	0±0	42	0±0
Sipunculida	7±7	0	26±18	42	35±26
Unknown	0±0	0	17±17	0	196±174
Total macrofauna	57,253±7876	4669	6605±333	39,088	24,566±3071

with mean densities of 9200 and 9500 individuals m^{-2}, respectively. Together these five taxa made up 90% of the individuals within the ampharetid-bed community.

The ampharetids formed tubes that extended > 10 cm into the sediment, but 92% of the individuals sampled were found in the top 5 cm of sediment (Fig. 3). The majority of the community was composed of surface-deposit feeders, including the ampharetids themselves. Sixty percent of the community was collected in the 0–1 cm fraction. Yet, ampharetids, as well as cumaceans and gammarid amphipods, were also found deep in the sediment; in the case of the ampharetids, 0.4% of individuals were found deeper than 10 cm. At the surface, the dorvilleids were not as abundant as either the gammarid amphipods or cumaceans but surpassed all but the ampharetids in density in the deeper layers; they were the second most abundant taxon between 1 and 5 cm depth (Fig. 3). Spionids were relatively evenly distributed throughout the sediment column and were not limited to the surface.

Group D_c had the second highest total assemblage and ampharetid density (Table 3). The density of Group D_c was 39,000 individuals m^{-2} including a high abundance of dorvilleid and paraonid polychaetes.

Groups B_c, C_c, and E_c were characterized by less dense assemblages. Group E_c had the third highest density, with a mean of 25,000 individuals m^{-2} and was mostly made up of spionid polychaetes and gammarid amphipods, with far reduced ampharetid and dorvilleid densities compared to Group A_c (Tables 2, 3). Groups B_c and C_c had the lowest macrofaunal density, between 4700 and 7200 individuals m^{-2}, and differed from each other due to higher abundance of oweniid polychaetes and small sponges in Group B_c and tanaids in Group C_c (Table 2). Group B_c consisted of Sta. 260, the off-seep station, and had the lowest density of all the samples collected with only 4700 individuals m^{-2}.

FA distribution—The 47 FAs that were identified included photosynthetic biomarkers (22:6(n-3); 20:5(n-3); 20:4(n-6); Dalsgaard et al. 2003), sulfate-reducer biomarkers (16:1(n-5); Elvert et al. 2003), and aerobic methanotrophic biomarkers (16:1(n-8); 16:1(n-6); Bowman et al. 1991; Tables 4, 5). Classification by FA analysis yielded four significantly different diet groups (labeled W_{FA}, X_{FA}, Y_{FA}, and Z_{FA}; Fig. 4; Table 4). The main difference between Group Y_{FA} and the remaining groups were the phytoplanktonic biomarkers 22:6(n-3) and 20:5(n-3). Group Y_{FA} was the most distinct (Fig. 4), although the two-dimensional (2D) ordination (stress = 0.21) was not a particularly good representation of the groupings (stress values < 0.2 are considered to be good representations of the multidimensional data in two dimensions; Clark and Warwick 2001). Groups W_{FA} and Z_{FA} were separated by 16:0 and 18:0 FAs, neither of which are necessarily dietary derived, although 16:1(n-7) and 18:1(n-7) helped characterize and discriminate both of these groups. The aerobic methanotrophic biomarker 16:1(n-8) contributed to the greatest dissimilarity between Group X_{FA} and Groups W_{FA} and Z_{FA} (Table 4).

The FA-distinct groupings also had carbon isotopic signatures that were significantly different from each other in all but two of the pair-wise comparisons (ANOVA $F_{3,65} = 9.86$; $p < 0.01$). Group X_{FA} had $\delta^{13}C$ signatures that were lighter than those of the remaining three groups and Group Z_{FA} $\delta^{13}C$ values were lighter than those of Group Y_{FA}, although average $\delta^{13}C$ values of Group W_{FA} and Group X_{FA} and of Group W_{FA} and Group Y_{FA} were not different from each other. Together these lines of evidence

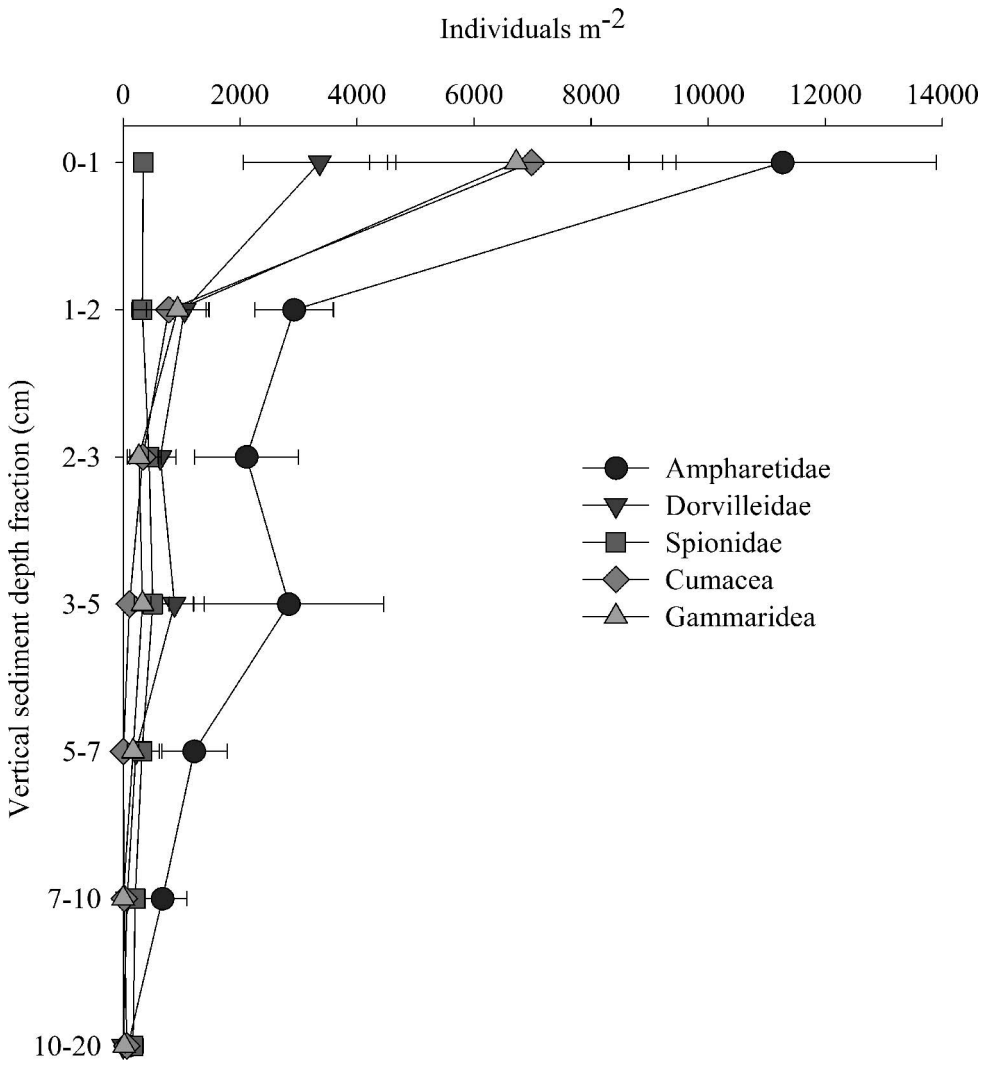

Fig. 3. Vertical distribution of dominant taxa within ampharetid-bed communities.

indicated that the FA composition differentiated groups that were mostly fueled by photosynthetic production from the remaining samples (Group Y_{FA} was different from all samples but Group W_{FA}) and that within the seep, aerobic methanotrophic biomarkers differentiated the grouping, separating those that had the lightest $\delta^{13}C$.

The aerobic methanotrophic biomarkers were present in 38 of the 69 FA samples analyzed, including all six of the sites and community groupings where FA samples were collected. The ubiquitous distribution of aerobic biomarkers supports the prevalence of aerobic methanotrophy throughout these sampling sites. Notably, even the Group Y_{FA} samples, which were collected from Sta. 46 and Sta. 84 and had fauna with a diet of mainly phytoplanktonic origin, also exhibited aerobic methanotrophic biomarker within their tissues.

The individuals that had similar FA signatures were diverse in their taxonomic lineages, and often single (putative) species spanned the FA groups (Fig. 4). Notably, the cumaceans were present in the group that had the greatest abundance of aerobic methanotrophic biomarkers (Group X_{FA}) as well Group Z_{FA}. In addition, the cumaceans had the most variable diet of all the species (Fig. 4; lower panel). *Ophryotrocha platykephale*, Ampharetid sp.1, and a variety of gammarid amphipod species were distributed in multiple of the significantly different groupings, indicating that they had divergent diets. Surprisingly, in the four species that were found in the Group Y_{FA} only the nemerteans, which we were not able to identify to species level, were also found in the other FA groupings. While we have included a sheath-forming bacterium, which is not macrofauna sensu stricto, within this FA comparison, its inclusion did not bias the relationship presented and thus we have left it in to identify where sheath-forming bacteria fall within our groupings.

Methane oxidation—By employing a biomass and carbon-based mixing model, one can estimate the amount of methane-derived carbon consumed by the ampharetid-bed community on a daily basis. Ampharetid-bed macrofaunal biomass was 201 g C m^{-2} (Sta. 261) and 273 g C m^{-2} (Sta. 196). Estimates for infaunal biomass derived from methane for the ampharetid-bed community were

Table 4. SIMPER results indicating which FAs characterized or discriminated the groupings identified in Fig. 4. Values indicate the contribution of the indicated FAs to the percent similarity or dissimilarity of the group. Total similarity or dissimilarity between groups is given in bold. Visualizations of the groupings are displayed in Fig. 4.

	Group W_{FA}		Group X_{FA}		Group Y_{FA}		Group Z_{FA}	
Group W_{FA}	**Σ Similarity**	**69**	**Σ Dissimilarity**	**41**	**Σ Dissimilarity**	**46**	**Σ Dissimilarity**	**43**
	16:0	16	16:1(n-8)	6	22:6(n-3)	8	20:1(n-13)	7
	18:1(n-7)	16	20:5(n-3)	5	20:4(n-6)	7	18:0	6
	20:5(n-3)	9	16:2a	5	20:1(n-13)	6	20:5(n-13)	6
	16:1(n-7)	9	16:0	5	18:0	5	22:1(n-9)	5
Group X_{FA}			**Σ Similarity**	**67**	**Σ Dissimilarity**	**48**	**Σ Dissimilarity**	**43**
			16:0	13	22:6(n-3)	7	16:1(n-8)	6
			16:1(n-7)	13	16:1(n-7)	6	16:1(n-7)	5
			18:1(n-7)	10	20:5(n-3)	6	16:2a	5
			18:0	8	16:1(n-8)	5	16:2b	5
Group Y_{FA}					**Σ Similarity**	**67**	**Σ Dissimilarity**	**43**
					16:0	15	22:6(n-3)	9
					20:5(n-3)	13	20:5(n-3	8
					18:0	12	20:4(n-6)	7
					18:1(n-7)	10	20:0	5
Group Z_{FA}							**Σ Similarity**	**66**
							16:0	21
							18:0	15
							18:1(n-7)	13
							18:1(n-9)	9

82–160 g C m^{-2} and 139–255 g C m^{-2} methane-derived carbon at Sta. 261 and Sta. 196, respectively. We can then employ the aforementioned respiration rate and respiratory quotient to conservatively estimate that the ampharetid-bed community consumed between 29 to 90 mmol C m^{-2} d^{-1} fixed by methanotrophic bacteria or Archaea.

Discussion

A novel seep community—The variety of habitats induced by geochemical heterogeneity at methane seeps increases the overall biodiversity on continental margins (Cordes et al. 2010). Identifying novel seep communities helps not only to characterize diversity, but to provide insight into the underlying mechanisms that drive biodiversity. The N.Z. ampharetid beds formed a distinct seep community on the N.Z. margin. Independent of site or location, those samples that contained abundant ampharetid polychaetes had a distinct assemblage structure due to the ampharetids themselves and to dorvilleid polychaetes; these two taxa typify other seep communities, especially microbial mat communities (Sahling et al. 2002; Bernardino et al. 2012; Levin et al. 2013). Ampharetids also differentiate seep community structure in other locations (Menot et al. 2010) and are commonly the most abundant infauna at seeps (Bernardino and Smith 2010; Menot et al. 2010; Ritt et al. 2010). However, in comparison to these other locations the density of fauna within the N.Z. ampharetid beds is far greater (Fig. 5). If we include mud volcanoes in this comparison, then only Håkon Mosby Mud Volcano has a denser community (93,000 individuals m^{-2}; that community was dominated by gastropods and tanaids; Decker et al. 2012). Although only the extreme cases of biomass were measured for the ampharetid beds, the community had greater biomass than any heterotrophic community from soft-sediment seeps currently known (Fig. 6). When looking at similar extreme values from other studies, the next highest heterotrophic biomass sample was a single microbial mat core from Hydrate Ridge that contained 199 g m^{-2} wet-weight biomass of which 191 g m^{-2} were Nuculandiae bivalves, a species that is not thought to contain symbionts (Sahling et al. 2002). With the inclusion of mud volcanoes and symbiont-bearing fauna, greater biomass has been observed than our maximum estimates of biomass, for example at the Napoli Mud Volcano (4.7 kg m^{-2}; Ritt et al. 2012; Fig. 6) and in the siboglinid fields at the Håkon Mosby Mud Volcano (1–2 kg m^{-2}; Niemann et al. 2006). Therefore, the ampharetid-bed density and biomass of N.Z. are potentially similar to that of mud volcanoes, and at the upper end of seeps in general. Canyons on the N.Z. margin can exhibit incredibly high benthic biomass driven by terrestrial inputs (1.3 kg megafauna m^{-2}; De Leo et al. 2010); however, the isotopic (Thurber et al. 2010) and FA composition (this study) from within the ampharetid beds demonstrate that neither surface nor terrestrial productivity of this region drive the high seep infaunal abundance and density.

We hypothesize that the abundant oxygen in the water column (relative to upwelling regions) combined with the bioirrigation of the ampharetids and high fluxes of methane lead to high densities and biomass. In contrast to areas such as Hydrate Ridge, Oregon, and Eel River, California, which occur either within or below oxygen minimum zones and have bottom water concentrations < 0.5 mL L^{-1} (Levin et al. 2010), New Zealand's margin is bathed in water with oxygen concentrations of 4.5 mL L^{-1} (Sommer et al. 2010). The type of fauna within a community can provide insight into the role of oxygen in structuring that

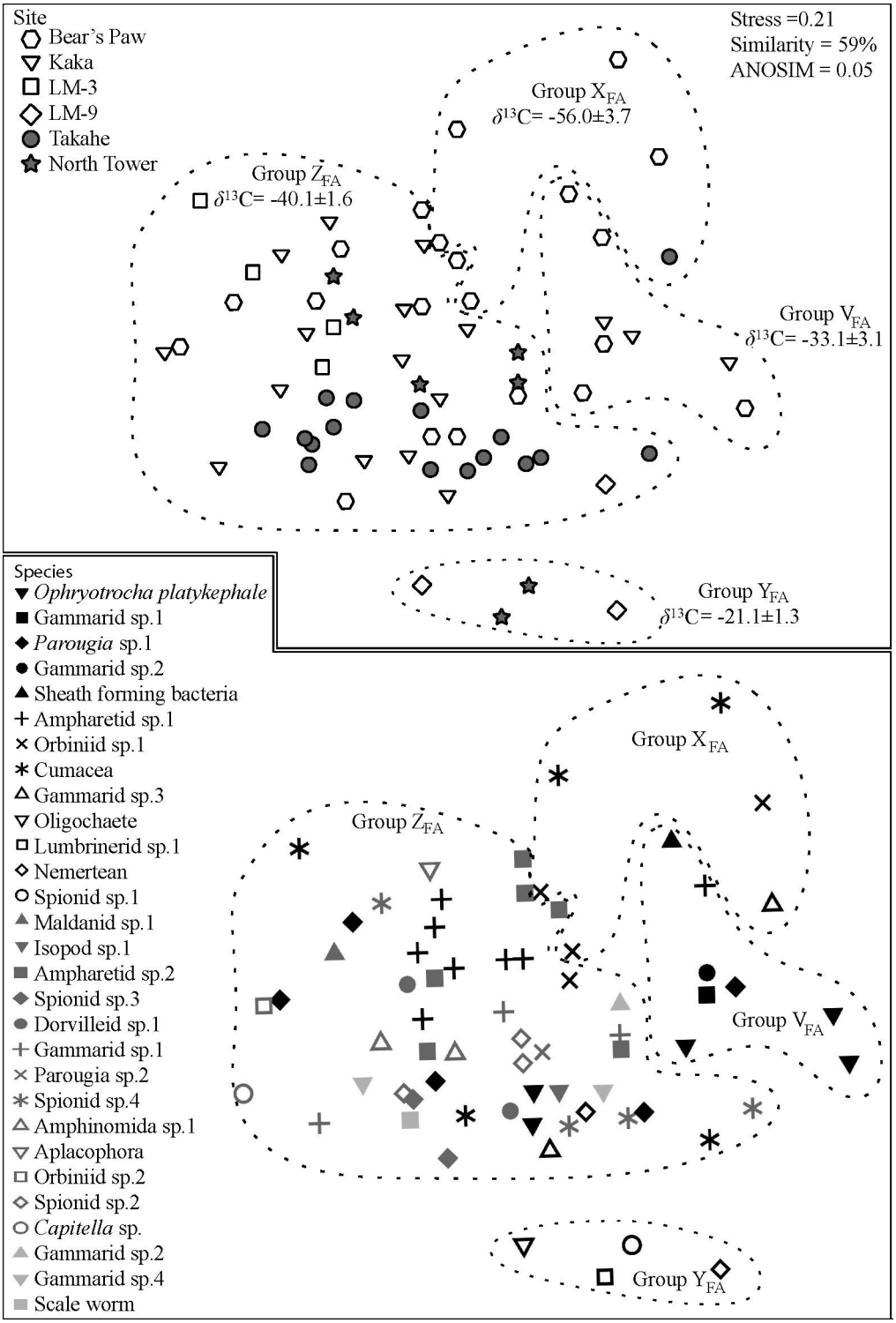

Fig. 4. A 2D representation of the similarity among FA profiles of individuals collected both within and outside of ampharetid beds. Significantly different groupings using the similarity cut off of 59% and an analysis of similarity (ANOSIM) with an $\alpha = 0.05\%$ are indicated by dotted lines. Mean isotopic composition for each group are given. Those FAs that drive the groupings are reported in Table 3. While the upper and lower panels are displaying the same MDS, the upper figure indicates the sites that the species were collected from and the lower panel indicates the species of the individual that was analyzed to provide each FA profile.

Table 5. Fatty acid (FA) and stable isotopic composition of each of the different FA clusters. Percentage of FA is given for those FAs which made up > 1% in any sample. Bold indicates aerobic methanotroph biomarkers, italics indicates sulfate-reducing bacteria biomarkers, and ***underlining*** indicates phytoplanktonic biomarkers. Letters a–d indicate different FAs which bond or branching pattern was not resolved. Footnote indicates the species whose FA profile were included in each group. Asterisk indicates likely FA identity.

	Group W_{FA}	Group X_{FA}	Group Y_{FA}	Group Z_{FA}
$\delta^{13}C$	−33.2±3.1	−56.0±3.7	−21.1±1.3	−40.9±1.6
14:0	2.3±0.6	2.0±0.4	1.4±1.0	3.0±0.4
14Ca	0.0±0.0	0.1±0.1	0.5±0.3	0.0±0.0
14Cb	0.0±0.0	0.0±0.0	0.4±0.4	0.0±0.0
i15	0.1±0.1	0.0±0.0	0.0±0.0	0.1±0.1
a15	0.0±0.0	0.1±0.1	0.0±0.0	0.0±0.0
15:0	0.3±0.2	0.3±0.1	1.1±0.2	0.2±0.1
16:1a	0.5±0.3	3.4±1.2	0.0±0.0	0.1±0.0
16:1(n-8)	**0.4±0.3**	**4.9±1.0**	**0.4±0.3**	**0.3±0.1**
16:1(n-7)	6.2±1.4	14.3±1.5	1.9±0.6	4.2±0.5
16:1(n-6)	**0.6±0.3**	**0.6±0.6**	**0.0±0.0**	**0.1±0.0**
16:2a	1.1±0.5	3.6±1.1	0.0±0.0	0.4±0.1
16:1(n-5)	*0.8±0.2*	*2.2±0.3*	*0.8±0.4*	*0.5±0.1*
16:2b	0.1±0.1	3.1±0.9	0.0±0.0	0.1±0.0
16:0	21.8±2.5	19.5±4.2	17.3±1.7	34.8±1.5
i16:1(n-5)*	0.0±0.0	0.1±0.0	0.0±0.0	0.2±0.1
i17:0	0.3±0.1	0.3±0.2	0.1±0.1	0.0±0.0
17:0	0.3±0.1	0.6±0.2	2.2±0.6	0.3±0.1
18:2a	0.1±0.1	0.1±0.1	0.0±0.0	0.1±0.0
18:2b	0.3±0.1	0.1±0.0	0.0±0.0	0.1±0.0
18:2(n-6)	1.9±0.4	1.0±0.2	0.6±0.3	0.9±0.1
18:1(n-9)	5.9±1.3	8.0±3.7	6.3±3.8	5.9±0.8
18:3	0.0±0.0	0.8±0.6	0.0±0.0	0.1±0.1
18:1(n-7)	24.5±4.9	8.5±1.6	7.5±1.9	11.0±0.8
18:2c	4.5±2.0	2.5±0.5	0.5±0.2	1.4±0.3
18:1(n-5)	*5.1±2.1*	*0.9±0.3*	*1.0±0.5*	*2.1±0.4*
18:2d	0.3±0.1	0.6±0.4	0.0±0.0	0.2±0.1
18:0	3.0±0.7	7.7±2.0	13.6±4.5	12.8±0.6
cycl18w9,10	0.4±0.2	0.4±0.2	1.1±0.7	0.2±0.1
19:0	0.0±0.0	0.0±0.0	0.1±0.1	0.0±0.0
20:4(n-6)	***0.0±0.0***	***0.5±0.4***	***6.3±2.8***	***0.6±0.1***
20:5(n-3)	***8.3±1.6***	***3.4±1.9***	***15.6±4.8***	***3.9±0.6***
20:2(n-9)	0.7±0.3	0.2±0.1	0.1±0.1	0.0±0.0
20:3a	0.0±0.0	0.2±0.1	0.2±0.2	0.4±0.1
20:1(n-13)	3.9±0.9	2.1±1.0	0.0±0.0	0.0±0.0
20:1(n-9)	0.0±0.0	0.9±0.4	2.0±1.3	2.0±0.3
20:1a	3.5±0.5	0.6±0.2	4.2±2.4	1.3±0.2
20:2b	0.2±0.2	0.1±0.1	0.0±0.0	0.3±0.1
20:0	0.0±0.0	0.2±0.1	0.0±0.0	0.2±0.0
i15	0.0±0.0	0.1±0.1	0.4±0.2	0.1±0.0
Unknown	0.5±0.3	0.2±0.1	0.0±0.0	0.0±0.0
22:6(n-3)	***0.3±0.3***	***0.3±0.3***	***8.8±3.8***	***0.5±0.2***
20:2c	0.1±0.1	0.5±0.3	0.2±0.1	0.2±0.1
20:2d	0.6±0.2	1.9±0.9	2.6±1.4	3.4±0.8
Unknown	0.3±0.3	0.1±0.1	0.0±0.0	4.5±0.9
22:1(n-9)	0.0±0.0	2.2±1.3	0.5±0.3	2.5±0.3
cycl22	0.0±0.0	0.0±0.0	0.1±0.1	0.4±0.3
22:1a	0.0±0.0	0.0±0.0	0.5±0.3	0.1±0.0

Group W: Ampharetid sp. 1; *Ophryotrocha platykephale* (3); *Parougia* sp. 1; Gammarid sp. 1; Gammarid sp. 2; Sheath-forming bacteria. Group X: Cumacea (2); Gammarid sp. 3; Orbiniid sp.1 (3). Group Y: Lumbrinerid sp.1; Nemertean; Oligochaeta sp.1; Spionid sp.1. Group Z: Isopoda sp.1; Ampharetid sp. 2 (6); Ampharetid sp. 1 (7); Amphinomida sp. 1 (2); Aplacophora sp.1; *Capitella* sp.; Cumacea (3); Gammarid sp. 3; Maldanid sp.1; Spionid sp.2 (3); Nemertean; *O. platykephale* (2); Orbiniid sp.1: Orbiniid sp.2; *Parougia* sp. 1 (4); *Parougia* sp. 2; Dorvilleid sp. 1 (2); Spionid sp.3 (2); Gammarid sp. 1 (3); Scale worm; Gammarid sp. 2; Spionid sp.4 (4); Gammarid sp. 4 (2).

community. In N.Z. ampharetid beds, the abundance of peracarid crustaceans, including gammarid amphipods and cumaceans, taxa that are less common in areas with low oxygen (Levin 2003), suggested that oxygen stress was not a driver of the community or was ameliorated through an additional mechanism. These two taxa reached maximum densities of 25,000 individuals m^{-2} and 23,000 individuals m^{-2}, respectively, in N.Z. (Table 3). Only a few ampeliscid amphipods were present; this group is sometimes abundant at the lower limit of oxygen minimum zones (Levin 2003). The dense community at the Håkon Mosby Mud Volcano is also overlain by well-oxygenated water, providing further support to the idea that overlying oxygen can be a determining factor in the density of reducing habitat fauna as the Håkon Mosby Mud Volcano has the greatest density of seep fauna currently known.

If we compare the vertical distribution of N.Z. ampharetid-bed fauna with other habitats, we can gain insight into the potential role that bioirrigation may play. Only 8% of the macrofauna that live in microbial mats at Eel River (off California, U.S.A.) live below top 2 cm of the sediment; a distribution thought to be caused by the high (> 1 mmol L^{-1}) levels of sulfide in the sediment immediately below the sediment surface. This high level of sulfide is caused by the persistent methane flux which is greater in microbial mats compared to Eel River clam beds (Levin et al. 2003). Similar to clam beds at Eel River that have 29% of their macrofaunal community below 2 cm (Levin et al. 2003), N.Z. ampharetid beds had 26% of their fauna below 2 cm (Fig. 3). At Eel River this deeper distribution of fauna was thought, in part, to be a result of bioirrigation of the clams that reduced sulfide concentration. Unlike Eel River clam beds which have reduced fluid emission compared to microbial mats (Levin et al. 2003), ampharetid beds had the highest methane flux measured on the N.Z. margin (Sommer et al. 2010), further distinguishing the ampharetid-bed community structure and biogeochemistry from known habitats. The identity of the fauna found below the sediment surface provided additional evidence that bioirrigation was an important factor in driving the sediment community. Only bivalves and the dorvilleid family of polychaetes are found in abundance at sulfide concentrations > 1 mmol L^{-1} (Levin 2005; Levin et al. 2013). Yet amphipods, cumaceans, and ampharetid and spionid polychaetes were all found > 5 cm below the sediment surface in the ampharetid beds. In the only core that has data currently available, sulfide within the ampharetid beds reached near 1 mmol L^{-1} within the top centimeter and after dropping to near 0 mmol L^{-1} increased to 3 mmol L^{-1} at 4 cm sediment depth (Dale et al. 2010). These sulfide values are much greater than we would expect to be tolerated by the fauna that we found occurring at those sediment depths unless sulfide and oxygen stress were mitigated.

In addition to affecting the distribution of metazoan fauna, bioirrigation and bioturbation can have profound

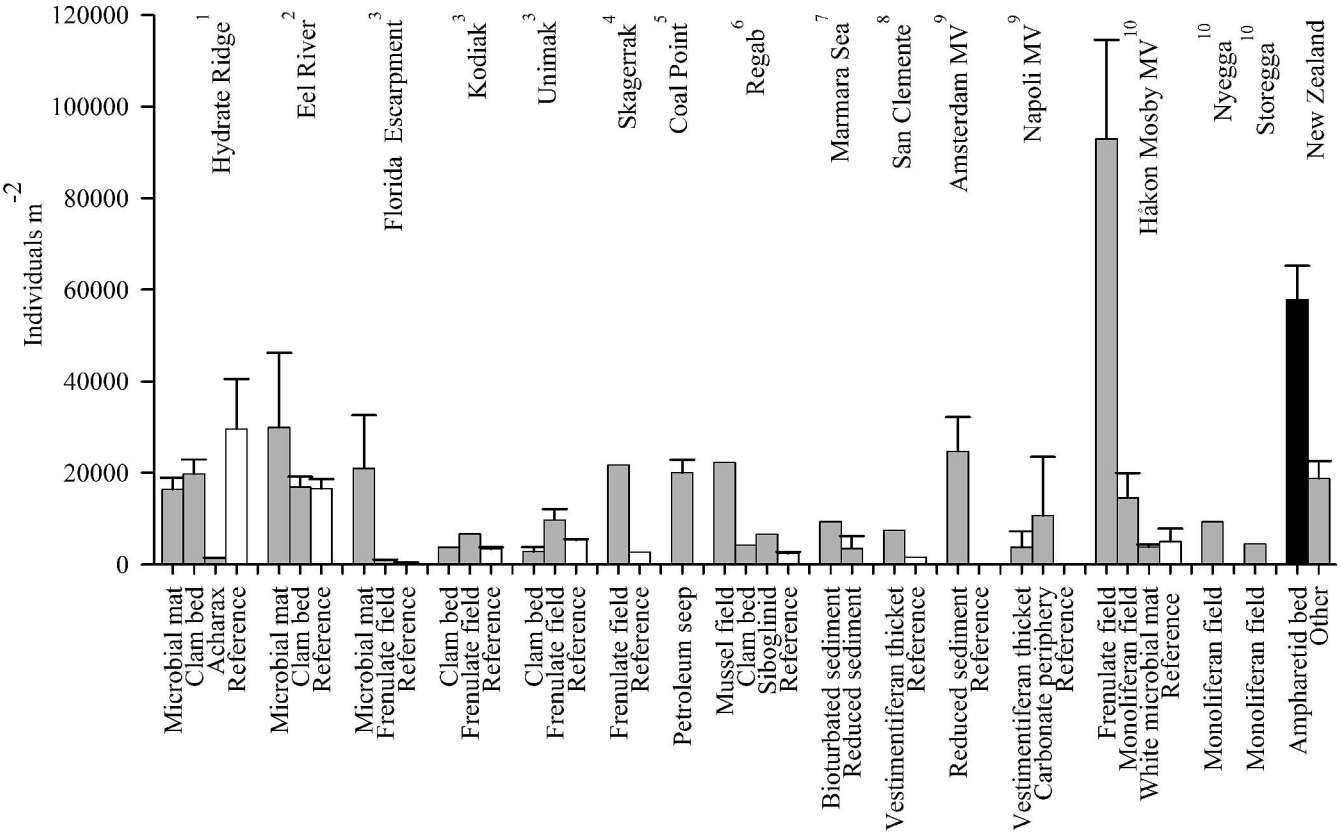

Fig. 5. Ampharetid-bed macrofaunal abundance compared to other methane seep communities and three mud volcano (MV) communities. Data from: [1]Levin et al. (2010) except for "Acharax," which is from Sahling et al. (2002); [2]Levin et al. 2003, 2006; [3]Levin and Mendoza 2007; [4]Dando et al. 1994; [5]Davis and Spies 1980; [6]Menot et al. 2010; [7]Ritt et al. 2010; [8]Bernardino and Smith 2010; [9]Ritt et al. 2012; [10]Decker et al. 2012.

effects on microbial sediment processes (Neilsen et al. 2004) and lead to increased food resources for metazoan fauna (Reichardt 1988). This role of bioirrigation in seep sediments is best known for clam beds where the clams stimulate sulfate reduction (Wallman et al. 1997) but in shallower sediments the distribution of oxygen and nitrate (Reichardt 1988) in addition to sulfate (Bertics and Ziebis 2010) are affected by bioturbation and bioirrigation. Shallow-water macrofauna use bioirrigation to cultivate bacteria within their burrow walls, leading to increased carbon fixation through hypothesized nitrogen-based chemoautotrophic production (Reichardt 1988). Although ampharetids form tubes rather than burrows, the role of the increased surface area caused by their tubes may favor aerobic processes, especially in light of the high water-column oxygen content. Thus, in addition to affecting the metazoan community distribution, the N.Z. macrofauna likely affect the microbial community type and distribution within the sediment. In non-seep sediments, dense assemblages of sipunculans (Graf 1989) and large tube-building maldanid polychaetes (Levin et al. 1997) are recognized as keystone resource modifiers—stimulating microbial activity and enhancing densities of other macrofauna deep in the sediment. These taxa become facilitators through downward transport of organic matter and oxygen, whereas the ampharetids may stimulate activity by conducting methane upward and oxygen downward.

Aerobic methanotrophy—Three separate approaches all yielded similar estimates of carbon demand for ampharetid-bed macrofauna. Our conservative species-specific mixing model projected minimum daily methanotroph carbon consumed by these infaunal communities to be 29 or 46 mmol C m^{-2} d^{-1}. Using a numerical-modeling approach based on sediment geochemical analysis of a single sample, Dale et al. (2010) estimated that the ampharetids within ampharetid beds used 23.2 mmol carbon m^{-2} d^{-1} from sources other than surface production or sulfide-oxidizing bacteria. By scaling up respiration based on density rather than biomass, Sommer et al. (2010) estimated that the oxygen requirements of the ampharetid-bed macrofauna was 30.8 mmol O_2 m^{-2} d^{-1}. In addition, in situ respiration chambers measured a maximum sediment community total oxygen utilization rate for ampharetid beds of 117 mmol m^{-2} d^{-1} (Fig. 7; Sommer et al. 2010) which is sufficient to cover the estimated or modeled carbon utilization rate from each of these approaches. Our estimates were based on the second (Sta. 261) and third (Sta. 196) most dense samples of ampharetid beds within this study as only those samples provided enough isotopic data to estimate the total methane consumed using our

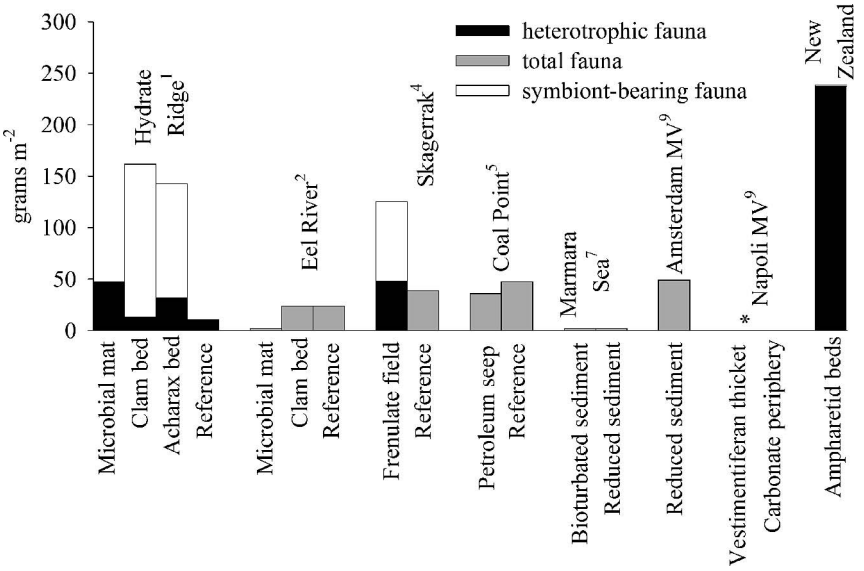

Fig. 6. Wet-weight biomass of ampharetid-bed communities from N.Z. in comparison to mean biomass from other seep infaunal communities and two mud volcano (MV) communities. Gray bars indicate a combination of heterotrophic and symbiont-bearing (chemosynthetic) fauna. Citations are the same as in Fig. 5 with the exception that footnote "1" is from Sahling et al. 2002. The asterisk indicates that the total biomass of this community was 4730 g, including large symbiont-bearing vestimentiferans that dominated the mass.

mixing-model approach (Table 1). While analyzing only two samples limits our ability to apply our findings to all ampharetid beds, as we cannot quantify the variance among ampharetid beds, the approximate agreement of our estimates with the approaches of Dale et al. (2010) and Sommer et al. (2010), suggests that our estimates probably do characterize the ampharetid-bed community carbon requirements.

Each of the estimates of ampharetid-bed oxygen and carbon requirement indicate that the rate of anaerobic methane oxidation measured (17 mmol C m^{-2} d^{-1}; Sommer et al. 2010) was insufficient to cover the demand of this macrofaunal community. The anaerobic methane-oxidizing consortia growth rate was only 0.1 mmol C m^{-2} d^{-1} (Fig. 7; Sommer et al. 2010), but to support the metazoan community through anaerobic methanotrophy, the entire anaerobic methane-oxidizing (AOM) population would have to double twice a day, an estimate that is 290 times greater than the observed growth rate. Although sulfate-reducer biomarkers were present in macrofaunal tissue, providing indications that part of the AOM consortia might be consumed, anaerobic processes were not sufficient to supply the observed methane-derived carbon requirements of macrofaunal biomass within the ampharetid beds.

Biomarkers provided support for aerobic methane oxidation as the main source of nutrition for the ampharetid-bed community. The FAs present within this community included both 16:1(n-6) and 16:1(n-8) that are found in Type I aerobic methanotrophs (Bowman et al. 1991). In addition, 16:1(n-8) helped to discriminate among the FA groupings, matching the lightest carbon isotopic signature that was found in Group X_{FA} (Fig. 4). Groups W_{FA} and Z_{FA} of the FA analysis had a diversity of biomarkers present, indicating that they were fed by a combination of seep bacteria including sulfide oxidizers, sulfate reducers, and aerobic methanotrophs. While the sum of (n-5) FAs has been indicative of archivory in other systems (Thurber et al. 2012), in the ampharetid beds its concentration did not match to isotopic values that would be indicative of methanotroph consumption. The concentration of aerobic methanotrophic biomarkers also differentiated Group X_{FA} from the other three groups; many of the individuals analyzed had these biomarkers, just not to the same high degree as those individuals whose FA profile resulted in their inclusion in Group X_{FA}. The clear reliance on methane-based biomass from the isotopic analysis combined with the abundance of aerobic methanotrophic biomarkers suggest that members of the ampharetid-bed community consume predominantly aerobic methanotrophs, but the diversity of other biomarkers indicate that this community is not composed of species that are aerobic methanotroph specialists. Both modeling (Dale et al. 2010) and benthic-chamber respiration rates (Sommer et al. 2010) identified missing carbon which they hypothesized could be filled by aerobic methanotrophy; this study is the first to provide conclusive evidence that this community was fueled by aerobic methanotrophy.

Of special note, ampharetids were not the only group that consumed aerobic methanotrophic biomass; the greatest amount of the aerobic methanotrophic biomarkers were found within orbiniid polychaetes, cumaceans, and a species of amphipod (*see* Table 5). The cumaceans were of particular interest, as the same species was present in multiple FA groups (including X_{FA} and Y_{FA}), meaning that the patterns we see are not simply the result of different FA syntheses and degradation patterns. Benthic

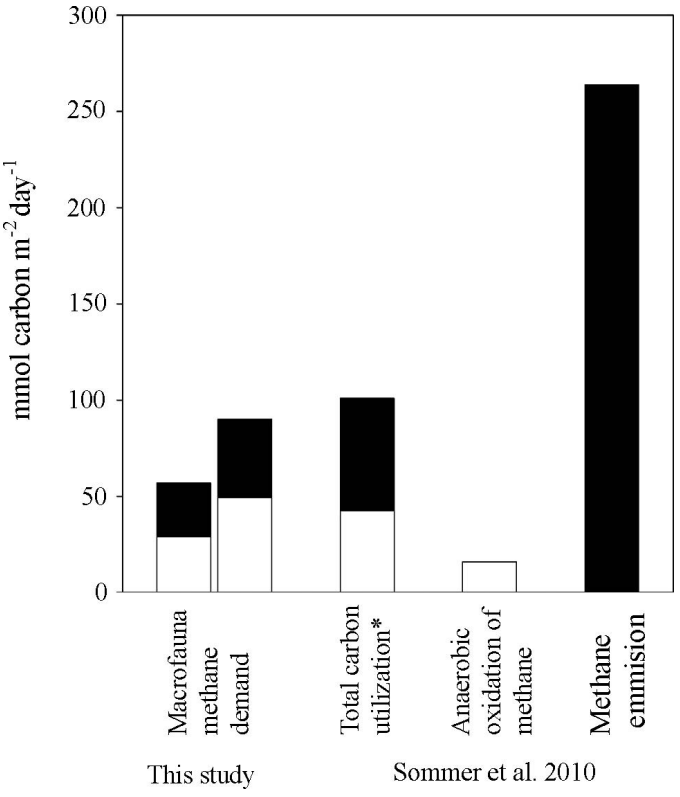

Fig. 7. Macrofaunal methane demand from two ampharetid beds in comparison to the total oxygen utilization, standing stock of anaerobic oxidation of methane (Note: growth rate was 0.1 mmol C m^{-2} d^{-1}), and maximum methane emission from ampharetid-bed communities. White bar indicates minimum estimate and the white bar plus the black bar indicates maximum conservative estimate. Total carbon utilization was calculated from total oxygen utilization from Sommer et al. (2010) using the respiratory quotient from Smith (1987).

consumers can synthesize a diversity of FAs, including a large proportion of their FA profile, thus presenting a great challenge in interpreting FA results (Kelly and Scheibling 2012). However, the ability to synthesize certain FAs is thought to follow taxonomic lineages (Bergé and Barnathan 2005) and having polychaetes and a diversity of arthropods, each belonging to all of the FA identified diet groupings (Fig. 4), provides support that our results are not simply the results of differential de novo synthesis by different species.

It is possible that the ampharetids facilitate transfer of this chemosynthetic energy to the rest of the fauna, including the cumaceans, present within the beds, in a form of "trophic engineering." It remains unknown whether the underlying geological forcing favors aerobic processes due to high methane flux rates that exceed the capacity of anaerobic processes or whether the bioirrigation of the ampharetids drives the unexpected high aerobic methane oxidation rate.

Methane flux—The aerobic methanotroph–fueled ampharetid community co-occurred with the highest measures of methane flux reported to date. The methane flux, which reached a maximum of 264 mmol CH_4 m^{-2} d^{-1}, is more than double any measured methane emission currently known from seeps (Sommer et al. 2010). While this methane provided sufficient methane reactants to support the microbial growth used by the metazoan community (Fig. 7), this unique confluence of methane emission and aerobic methanotroph–fueled biomass raises the question of whether the consumption of these methanotrophs by ampharetids caused the increased methane release, either through top-down forcing on the aerobic methanotrophs themselves or by ampharetid tubes acting as conduits that, combined with bioirrigation, facilitate methane release from sediments into the water column.

Although the importance of aerobic methanotrophs in the methane cycle is not unique to N.Z. ampharetid beds, a dense metazoan community that consumes it is currently unique. In a recent study, > 40% of the microbial community within a hydrocarbon seep microbial mat at Coal Point (off California) was composed of aerobic methanotrophs, which had the same (n-6) and (n-8) biomarkers observed here (Ding and Valentine 2008). At Håkon Mosby Mud Volcano (Barents Sea), another well-oxygenated seep setting, nematodes consumed aerobic methanotrophic production (Van Gaever et al. 2009), yet only 1–3% of methane is oxidized aerobically at this seep site in contrast to 37% of methane being oxidized by anaerobic processes (Niemann et al. 2006; Reeburg 2007). In rice paddies, aerobic methanotrophs are preferentially grazed upon by protists (Murase and Frenzel 2007). Yet the incorporation of aerobic methanotrophic biomass by an entire community of metazoan fauna is heretofore novel. How consumption of aerobic methanotrophs affects the biogeochemical cycling and methane emission at each of these locations remains unknown. The N.Z. ampharetid beds, due to their increased methane emission, present an ideal system to study whether infauna consume the sediment filter and thus enhance the release of methane into the overlying water column and potentially the atmosphere.

Acknowledgments

We thank (in alphabetical order) Amy Baco, Carlos Neira, Olaf Pfannkuche, and Craig R. Smith for making this research possible and Jens Greinert, David Bowden, Angelo Bernardino, Helena Wiklund, and the captains, crews, and the remaining science parties of R/V *Tangaroa* (cruise TAN0616) and R/V *Sonne* (Cruise SO191-3) for additional assistance at sea. Lipid analysis was made possible due to the kind lending of instrument time by William Gerwick and the support of his laboratory, including Cameron Coates and Jo Nunnery. Jennifer Gonzalez assisted with the sorting of infauna and processing of isotope samples in the laboratory. Funding was provided by the Sidney E. Frank Foundation, Scripps Institution of Oceanography Graduate Office, Michael M. Mullin Memorial Fellowship, and the United States National Oceanic and Atmospheric Administration, Office of Exploration Grants NA17RJ1231 and NA050AR417076, United States National Science Foundation Grants OCE-0425317 and OCE-0826254, New Zealand Institute of Water and Atmospheric Research Capability Fund project CRFH073, and a University of California Academic Senate grant to L.A.L. and W. Gerwick. The Federal Ministry of Education and Research, Germany (grants 03Go600D and 03Go191A) provided R/V *Sonne* and additional grants for geochemical work. This

manuscript was greatly improved by the insight of two anonymous reviewers. This is publication number GEOTECH-2093.

References

Baco, A. R., A. A. Rowden, L. A. Levin, C. R. Smith, and D. A. Bowden. 2010. Initial characterization of cold seep faunal communities on the New Zealand Hikurangi margin. Mar. Geol. **272:** 251–259, doi:10.1016/j.margeo.2009.06.015

Barnes, P. M., and others. 2010. Tectonic and geological framework for gas hydrates and cold seeps on the Hikurangi subduction margin, New Zealand. Mar. Geol. **272:** 26–48, doi:10.1016/j.margeo.2009.03.012

Bergé, J. P., and G. Barnathan. 2005. Fatty acids from lipids of marine organisms: Molecular biodiversity, roles as biomarkers, biologically active compounds, and economical aspects. Mar. Biotechnol. I **96:** 49–125, doi:10.1007/b135782

Bernardino, A., and C. R. Smith. 2010. Community structure of infaunal macrobenthos around vestimentiferan thickets at the San Clemente cold seep, NE Pacific. Mar. Ecol. **31:** 608–621, doi:10.1111/j.1439-0485.2010.00389.x

Bernardino, A. F., L. A. Levin, A. R. Thurber, and C. R. Smith. 2012. Comparative composition, diversity and trophic ecology of sediment macrofauna at Vents, Seeps and Organic Falls. PLoS One **7:** e33515, doi:10.1371/journal.pone.0033515

Bertics, V. J., and W. Ziebis. 2010. Bioturbation and the role of microniches for sulfate reduction in coastal marine sediments. Environ. Microbiol. **12:** 3022–3034, doi:10.1111/j.1462-2920.2010.02279.x

Bowman, J. P., J. H. Skerratt, P. D. Nichols, and L. I. Sly. 1991. Phospholipid fatty acid and lipopolysaccharide fatty acid signature lipids in methane-utilizing bacteria. FEMS Microbiol. Ecol. **85:** 15–22, doi:10.1111/j.1574-6968.1991.tb04693.x

Clarke, K. R., and R. N. Gorley. 2006. PRIMER v6. User manual and tutorial. PRIMER-E.

———, P. J. Somerfield, and R. N. Gorley. 2008. Testing of null hypotheses in exploratory community analyses: Similarity profiles and biota-environment linkage. J. Mar. Exp. Biol. **366:** 56–69, doi:10.1016/j.jembe.2008.07.009

———, and R. M. Warwick. 2001. Change in marine communities: an approach to statistical analysis and interpretation (2nd Edition). PRIMER-E.

Cordes, E. E., and others. 2010. The influence of geological, geochemical, and biogenic habitat heterogeneity on seep biodiversity. Mar. Ecol. **31:** 51–65, doi:10.1111/j.1439-0485.2009.00334.x

Dale, A. W., S. Sommer, M. Haeckel, K. Wallmann, P. Linke, G. Wegener, and O. Pfannkuche. 2010. Pathways and regulation of carbon, sulfur, and energy transfer in marine sediments overlying methane gas hydrates on the Opouawe Bank (New Zealand). Geochim. Cosmochim. Acta **74:** 5763–5784, doi:10.1016/j.gca.2010.06.038

Dalsgaard, J., M. St. John, G. Kattner, D. Müller-Navarra, and W. Hagen. 2003. Fatty acid trophic markers in the pelagic marine environment. Adv. Mar. Biol. **46:** 225–340, doi:10.1016/S0065-2881(03)46005-7

Dando, P. R., I. Bussmann, S. J. Niven, S. C. M. O'hara, R. Schmaljohann, and L. J. Taylor. 1994. A methane seep area in the Skagerrak, the habitat of the pogonophore *Siboglinum poseidoni* and the bivalve mollusc *Thyasira sarsi*. Mar. Ecol. Progr. Ser. **107:** 157–167, doi:10.3354/meps107157

Dattagupta, S., M. A. Arther, and C. R. Fisher. 2008. Modification of sediment geochemistry by the hydrocarbon seep tubeworm *Lamellibrachia luymesi:* A combined empirical and modeling approach. Geochim. Cosmochim. Acta **72:** 2298–2315, doi:10.1016/j.gca.2008.02.016

Davis, P. H., and R. B. Spies. 1980. Infaunal benthos of a natural petroleum seep: Study of community structure. Mar. Biol. **59:** 31–41, doi:10.1007/BF00396980

De Leo, F. C., C. R. Smith, A. A. Rowden, D. A. Bowden, and M. R. Clark. 2010. Submarine canyons: Hotspots of benthic biodiversity and productivity in the deep sea. Proc. R. Soc. B **277:** 2783–2792, doi:10.1098/rspb.2010.0462

Decker, C., and others. 2012. Habitat heterogeneity influences cold-seep macrofaunal communities within and among seeps along the Norwegian margin. Part 1: Macrofaunal community structure. Mar. Ecol. **33:** 205–230, doi:10.1111/j.1439-0485.2011.00503.x

Deines, P., P. L. E. Bodelier, and G. Eller. 2007. Methane-derived carbon flows through methane-oxidizing bacteria to higher trophic levels in aquatic systems. Environ. Microbiol. **9:** 1126–1134, doi:10.1111/j.1462-2920.2006.01235.x

Ding, H., and D. L. Valentine. 2008. Methanotrophic bacteria occupy benthic microbial mats in shallow marine hydrocarbon seeps, Coal Oil Point, California. J. Geo. Res. **113:** 1–11, doi:10.1029/2008JA013037

Eller, G., P. Deines, J. Grey, H.-H. Richnow, and M. Krüger. 2005. Methane cycling in lake sediments and its influence on chironomid larval $\delta^{13}C$. FEMS Microb. Ecol. **54**: 339–350, doi:10.1016/j.femsec.2005.04.006

Elvert, M., A. Boetius, K. Knittel, and B. B. Jørgensen. 2003. Characterization of specific membrane fatty acids as chemotaxonomic markers for sulfate-reducing bacteria involved in anaerobic oxidation of methane. Geomicrobiol. J. **20:** 403–419, doi:10.1080/01490450303894

Fry, B., and E. B. Sherr. 1984. $\delta^{13}C$ measurements as indicators of carbon flow in marine and freshwater systems. Contrib. Mar. Sci. **27:** 13–46.

Graf, G. 1989. Bentho-pelagic coupling in a deep-sea benthic community. Nature **341:** 437–439, doi:10.1038/341437a0

Greinert, J., and others. 2010. Methane seepage along the Hikurangi margin, New Zealand: Overview of studies in 2006 and 2007 and new evidence from visual, bathymetric and hydroacoustic investigations. Mar. Geol. **272:** 6–25, doi:10.1016/j.margeo.2010.01.017

Kelly, J. R., and R. E. Scheibling. 2012. Fatty acids as dietary tracers in benthic food webs. Mar. Ecol. Prog. Ser. **446:** 1–22, doi:10.3354/meps09559

Knittel, K., and A. Boetius. 2009. Anaerobic oxidation of methane: Progress with an unknown process. Annu. Rev. Microbiol. **63:** 311–334, doi:10.1146/annurev.micro.61.080706.093130

Levin, L. A. 2003. Oxygen minimum zone benthos: Adaptation and community response to hypoxia. Oceanogr. Mar. Biol. Annu. Rev. **41:** 1–45.

———. 2005. Ecology of cold seep sediments: Interactions of fauna with flow, chemistry and microbes. Oceanogr. Mar. Biol. Annu. Rev. **43:** 1–46, doi:10.1201/9781420037449.ch1

———, N. Blair, D. DeMaster, G. Plaia, W. Fornes, C. Martin, and C. Thomas. 1997. Rapid subduction of organic matter by maldanid polychaetes on the North Carolina slope. J. Mar. Res. **55:** 595–611, doi:10.1357/0022240973224337

———, and G. F. Mendoza. 2007. Community structure and nutrition of deep methane-seep macrobenthos from the North Pacific (Aleutian) Margin and the Gulf of Mexico (Florida Escarpment). Marine Ecology **28:** 131–151, doi:10.1111/j.1439-0485.2007.00153.x

———, ———, J. P. Gonzalez, A. R. Thurber, and E. E. Cordes. 2010. Diversity of bathyal macrofauna on the northeastern Pacific margin: The influence of methane seeps and oxygen minimum zones. Mar. Ecol. **31:** 94–110, doi:10.1111/j.1439-0485.2009.00335.x

———, W. Ziebis, G. F. Mendoza, V. Growney-Cannon, and S. Walther. 2006. Recruitment response of methane-seep macrofauna to sulfide-rich sediments: An in situ experiment. J. Exp. Mar. Biol. Ecol. **330:** 132–150, doi:10.1016/j.jembe.2005.12.022

———, and others. 2003. Spatial heterogeneity of macrofauna at northern California methane seeps: The influence of sulfide concentration and fluid flow. Mar. Ecol. Prog. Ser. **265:** 123–139, doi:10.3354/meps265123

———, and ———. 2013. Ecological release and niche partitioning under stress: Lessons from dorvilleid polychaetes in sulphidic sediments at methane seeps. Deep-Sea Res II **92:** 214–233, doi:10.1016/j.dsr2.2013.02.006

Lewis, T., P. D. Nichols, and T. A. McMeekin. 2000. Evaluation of extraction methods for recovery of fatty acids from lipid-producing microheterotrophs. J. Microbiol. Methods **43:** 107–116, doi:10.1016/S0167-7012(00)00217-7

MacAvoy, S. E., S. A. Macko, and R. S. Carney. 2003. Links between chemosynthetic production and mobile predators on the Louisiana continental slope: Stable carbon isotopes of specific fatty acids. Chem. Geol. **201:** 229–237, doi:10.1016/S0009-2541(03)00204-3

Menot, L., J. Galéron, K. Olu, J.-C. Caprais, P. Crassous, A. Khripounoff, and M. Sibuet. 2010. Spatial heterogeneity of macrofaunal communities in and near a giant pockmark area in the deep Gulf of Guinea. Mar. Ecol. **31:** 78–93, doi:10.1111/j.1439-0485.2009.00340.x

Murase, J., and P. Frenzel. 2007. A methane-driven microbial food web in a wetland rice soil. Environ. Microbiol. **9:** 3025–3034, doi:10.1111/j.1462-2920.2007.01414.x

Nielsen, O. I., B. Gribsholt, E. Kristensen, and N. P. Revsbech. 2004. Microscale distribution of oxygen and nitrate in sediment inhabited by *Nereis diversicolor*: spatial patterns and estimated reaction rates. Aquat. Microb. Ecol. **34:** 23–32, doi:10.3354/ame034023

Niemann, H., and others. 2006. Novel microbial communities of the Håkon Mosby mud volcano and their role as a methane sink. Nature **443:** 854–858, doi:10.1038/nature05227

Reeburg, W. S. 2007. Ocean marine biogeochemistry. Chem. Rev. **107:** 486–513, doi:10.1021/cr050362v

Reichardt, W. 1988. Impact of bioturbation by *Arenicola marina* on microbiological parameters in intertidal sediments. Mar. Ecol. Prog. Ser. **44:** 149–158, doi:10.3354/meps044149

Ritt, B., and others. 2010. First insights into the structure and environmental setting of cold-seep communities in the Marmara Sea. Deep-Sea Res. I **57:** 1120–1136, doi:10.1016/j.dsr.2010.05.011

———, and ———. 2012. Seep communities from two mud volcanoes in the deep eastern Mediterranean Sea: Faunal composition, spatial patterns and environmental control. Mar. Ecol. Prog. Ser. **466:** 93–119, doi:10.3354/meps09896

Sahling, H., D. Richert, R. W. Lee, P. Linke, and E. Suess. 2002. Macrofaunal community structure and sulfide flux at gas hydrate deposits from the Cascadia convergent margin, NE Pacific. Mar. Ecol. Prog. Ser. **231:** 121–138, doi:10.3354/meps231121

Smith, K. L. 1987. Food energy supply and demand: A discrepancy between particulate organic carbon flux and sediment community oxygen consumption in the deep ocean. Limnol. Oceanogr. **32:** 201–220, doi:10.4319/lo.1987.32.1.0201

Somero, G. N., J. J. Childress, and A. E. Anderson. 1989. Transport, metabolism, and detoxification of hydrogen sulfide in animals from sulfide-rich marine environments. Aquat. Sci. **1:** 591–614.

Sommer, S., P. Linke, O. Pfannkuche, H. Niemann, and T. Treude. 2010. Benthic respiration in a seep habitat dominated by dense beds of ampharetid polychaetes at the Hikurangi Margin (New Zealand). Mar. Geol. **272:** 223–232, doi:10.1016/j.margeo.2009.06.003

———, and others. 2006. Efficiency of the benthic filter: Biological control of emission of dissolved methane from sediments containing shallow gas hydrates at Hydrate Ridge. Global Biogeochem. Cycles **20:** GB2019, doi:10.1029/2004GB002389

———, and ———. 2009. Seabed methane emission and the habitat of frenulate tubeworms on the Captain Arutyunov mud volcano (Gulf of Cadiz). Mar. Ecol. Prog. Ser. **382:** 69–86, doi:10.3354/meps07956

Thurber, A. R., K. Kröger, C. Neira, H. Wiklund, and L. A. Levin. 2010. Stable isotope signatures and methane use by New Zealand cold seep benthos. Mar. Geol. **272:** 260–269, doi:10.1016/j.margeo.2009.06.001

———, L. A. Levin, V. J. Orphan, and J. J. Marlow. 2012. Archaea in metazoan diets: Implications for food webs and biogeochemical cycling. ISME J. **6:** 1602–1612, doi:10.1038/ismej.2012.16

Tryon, M. D., and K. M. Brown. 2001. Complex flow patterns through Hydrate Ridge and their impact on seep biota. Geophys. Res. Lett. **28:** 2863–2866, doi:10.1029/2000GL012566

Van Dover, C. L., R. Michener, and K. Lajtha. 2007. Stable isotope studies in marine chemoautotrophically based ecosystems: An update, p. 202–237. *In* R. Michener and K. Lajtha [eds.], Stable isotopes in ecology and environmental science, 2nd ed. Blackwell.

Van Gaever, S., L. Moodley, F. Pasotti, M. Houtekamer, J. J. Middelburg, R. Danovaro, and A. Vanreusel. 2009. Trophic specialization of metazoan meiofauna at the Håkon Mosby Mud Volcano: Fatty acid biomarker isotope evidence. Mar. Biol. **156:** 1289–1296, doi:10.1007/s00227-009-1170-9

Wallmann, K., and others. 1997. Quantifying fluid flow, solute mixing, and biogeochemical turnover at cold vents of the eastern Aleutian subduction zone. Geochim. Cosmochim. Acta **24:** 5209–5219, doi:10.1016/S0016-7037(97)00306-2

Associate editor: Ronnie Nøhr Glud

Received: 20 February 2013
Accepted: 10 April 2013
Amended: 17 April 2013